Supporting Information

Wille *et al.* 10.1073/pnas.0812770106

SI Methods

SDS/PAGE, Silver Staining, and Western Blot Analysis. Protein samples were mixed with equal volumes of SDS-sample buffer, boiled for 5 min, and cooled on ice before loading 30- to 60-μL samples onto 15% SDS/PAGE gels. Silver staining of the gels was performed as described (1). The Western blots were incubated with anti-PrP recFab D18 (2) diluted 1:1,000 or anti-PrP polyclonal antiserum W5517 (Serban *et al.*, unpublished data). After extensive washing, the blots were incubated with peroxidase-labeled anti-mouse or anti-rabbit Fc secondary antibody (Pierce Biotechnology) and developed by the enhanced chemiluminescence (ECL) system (Amersham Life Sciences), as described (3).

Sandwich CDI for Mouse PrP^{Sc}. The CDI was performed with recFab D13 (4) labeled with Eu-chelate of *N*-(*p*-isothiocyanatobenzyl)-diethylenetriamine-N^1,N^2,N^3,N^3-tetraacetic acid at pH 8.5 for 16 h at RT as described (5). The principle, development, calibration, and calculation of PrP^{Sc} concentration from CDI data have been described (5, 6).

Preparation of 2D Crystals from PrP 27-30 (Traditional Method). PrP 27-30 was prepared from the brains of scrapie-sick, wild-type FVB mice infected with RML prions or Syrian hamsters infected with Sc237 prions. The purification was performed as published (7). The final step of the procedure consisted of a sucrose-gradient centrifugation. As previously described (8), some fractions of the sucrose gradient contained, in addition to the normally seen prion rods, 2D crystals. Because the 2D crystals originate in preparations that have high titers of infectivity and have not been treated by denaturing agents, these crystals are considered to be fully infectious. ImmunoGold labeling with several monoclonal antibodies against PrP confirmed that the 2D crystals contain PrP (9). Furthermore, the monoclonal antibody 3F4, which does not recognize PrP^{Sc} or PrP 27-30 but binds PrP^{C} and denatured PrP (5, 10–12), binds the 2D crystals only after denaturation; this finding argues that the 2D crystals are indeed formed from infectious PrP 27-30 (9).

Preparation of POM Stock Solutions. PTA and HTA were purchased from Aldrich, SiTA from City Chemical, and were used without further purification. BTA, TTA, and AsTA were prepared according to the reported procedures (13). In the case of BTA and TTA, the solubility of the complexes was increased by exchanging K^+ with Na^+. Stock solutions of 10–40% (wt/vol) POM were prepared by dissolving each POM in water, then neutralized with NaOH or LiOH to achieve a final pH of 7.4. The PTA/$MgCl_2$ solution (10% wt/vol) was prepared by dissolving 10 g of PTA and 1.73 g of $MgCl_2 \cdot 6H_2O$ in water, followed by neutralization with NaOH.

Image Processing. Images of well-ordered 2D crystals were taken at a calibrated magnification of 75,750×, which is equivalent to 1.98 Å per pixel. The image processing was completed essentially as described in refs. 8 and 9. In brief, the contrast transfer function (CTF) was corrected using the CRISP software package (14). CRISP was also used to compensate in part for the dampening of the CTF function at higher resolution. The CTF-corrected images were processed by using a single-particle approach by correlation-mapping a manually chosen 256 × 256 pixel reference onto the original image (15, 16). The resulting average was used in a rotational and translational search to align the individual subsets of the original image. Correlation-mapping and -averaging were completed by using routines written for the SPIDER and WEB software package (17). After 17 iterations, the algorithm converged and no further improvements could be achieved. The final correlation average was used for crystallographic analysis and averaging, again by using the CRISP software package (14). As seen before (8, 9), both the raw 2D crystals and the correlation averages showed clear p3 plane group symmetry, hence p3 symmetry was applied during crystallographic averaging.

Determining the Fibril and 2D Crystal Content of PrP 27-30 Preparations. To quantify the amount of amyloid-like fibrils in the PrP 27-30 preparations, 10 electron micrographs were taken at random positions. We took advantage of the PrP 27-30–POM interaction and used the positive contrast of the POM-decorated fibers for detection. Micrographs that contained large film defects, obvious dirt particles, and other artifacts were discarded and replaced. All images were taken at a low magnification (7,575× corresponding to 19.8 Å per pixel) and a higher than usual under-focus (5–10 μm) to facilitate the quantification. The electron micrographs were processed with Adobe Photoshop. In brief, the number of pixels (representing the area) for each visible particle in the electron micrographs was determined. Individual particles were selected by using the "magic wand" tool with a setting of 50–100; the Fresnel fringes caused by the strong under-focus made it easier to delineate each particle separately. The histogram menu provided the number of pixels for each particle. Particles were classified as fibrils if the length was >40 pixels, equivalent to ≈78 nm, and the length:width ratio was at least 2:1. The amount of fibrils was averaged over all 10 micrographs. The stochastic distribution of the fibrils on the support film is reflected in the relatively large standard errors of the mean (SEMs).

Statistical Analysis. To determine the statistical significance of the observed differences in the fibril and 2D crystal content, and of the ImmunoGold-labeled densities, we analyzed the data by using *t* tests. Before performing the *t* tests, we ascertained if the variance of the two datasets was comparable (*F* test). Depending on the outcome of the *F* test, we either used a homoscedastic *t* test assuming equal variances or a heteroscedastic *t* test allowing for unequal variances. Statistical significance was achieved if the *P* value for the 2-tailed *t* test was <0.05.

1. Merril CR, Dunau ML, Goldman D (1981) A rapid sensitive silver stain for polypeptides in polyacrylamide gels. *Anal Biochem* 110:201–207.
2. Williamson RA, *et al.* (1996) Circumventing tolerance to generate autologous monoclonal antibodies to the prion protein. *Proc Natl Acad Sci USA* 93:7279–7282.
3. Tremblay P, *et al.* (2004) Mutant PrP^{Sc} conformers induced by a synthetic peptide and several prion strains. *J Virol* 78:2088–2099.
4. Perrier V, *et al.* (2000) Mimicking dominant negative inhibition of prion replication through structure-based drug design. *Proc Natl Acad Sci USA* 97:6073–6078.
5. Safar J, *et al.* (1998) Eight prion strains have PrP^{Sc} molecules with different conformations. *Nat Med* 4:1157–1165.
6. Safar JG, *et al.* (2005) Diagnosis of human prion disease. *Proc Natl Acad Sci USA* 102:3501–3506.
7. Prusiner SB, *et al.* (1982) Further purification and characterization of scrapie prions. *Biochemistry* 21:6942–6950.
8. Wille H, *et al.* (2002) Structural studies of the scrapie prion protein by electron crystallography. *Proc Natl Acad Sci USA* 99:3563–3568.

9. Wille H, *et al.* (2007) Electron crystallography of the scrapie prion protein complexed with heavy metals. *Arch Biochem Biophys* 467:239–248.
10. Kascsak RJ, *et al.* (1987) Mouse polyclonal and monoclonal antibody to scrapie-associated fibril proteins. *J Virol* 61:3688–3693.
11. Rogers M, *et al.* (1991) Epitope mapping of the Syrian hamster prion protein utilizing chimeric and mutant genes in a vaccinia virus expression system. *J Immunol* 147:3568–3574.
12. Peretz D, *et al.* (1997) A conformational transition at the N-terminus of the prion protein features in formation of the scrapie isoform. *J Mol Biol* 273:614–622.
13. Lee IS, Long JR, Prusiner SB, Safar JG (2005) Selective precipitation of prions by polyoxometalate complexes. *J Am Chem Soc* 127:13802–13803.
14. Hovmöller S (1992) CRISP: Crystallographic image processing on a personal computer. *Ultramicroscopy* 41:121–135.
15. Crepeau RH, Fram EK (1981) Reconstruction of imperfectly ordered zinc-induced tubulin sheets using cross-correlation and real space averaging. *Ultramicroscopy* 6:7–17.
16. Frank J (1982) New methods for averaging non-periodic objects and distorted crystals in biologic electron microscopy. *Optik* 63:67–89.
17. Frank J, *et al.* (1996) SPIDER and WEB: Processing and visualization of images in 3D electron microscopy and related fields. *J Struct Biol* 116:190–199.

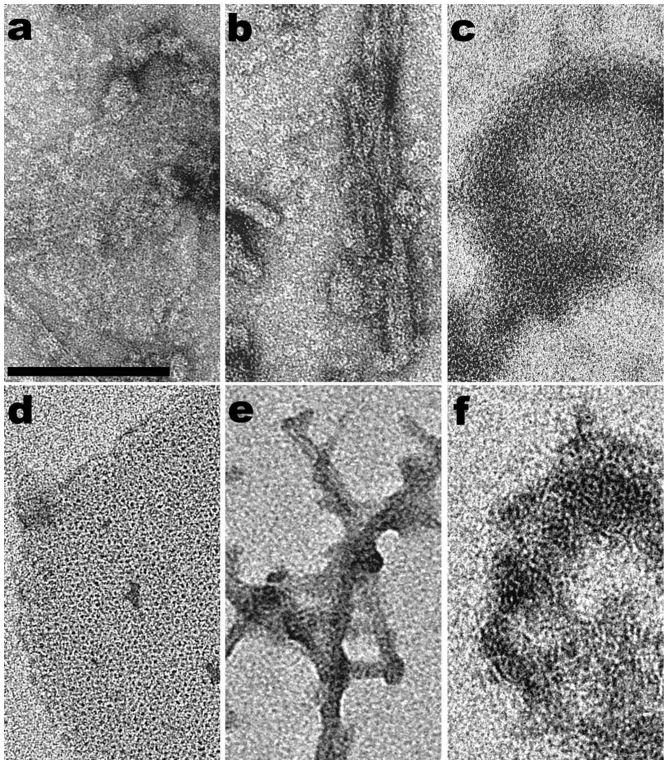

Fig. S1. Electron micrographs of 2D crystals and prion rods obtained by the traditional purification procedure (*a* and *b*) and by PTA precipitation (*d* and *e*). PrP 27-30 was prepared from RML-infected FVB brains. Samples prepared from uninoculated FVB control brains by the traditional purification procedure (*c*) and by PTA precipitation (*f*) show neither prion rods nor 2D crystals, but only amorphous aggregates and diffuse lipid structures. With the traditional purification protocol, the 2D crystals of PrP 27-30 were small and disordered (*a*), whereas those resulting from PTA precipitation were larger and relatively well ordered (*d*). (Scale bar: *a*, 100 nm; applies to *b*–*f*.)

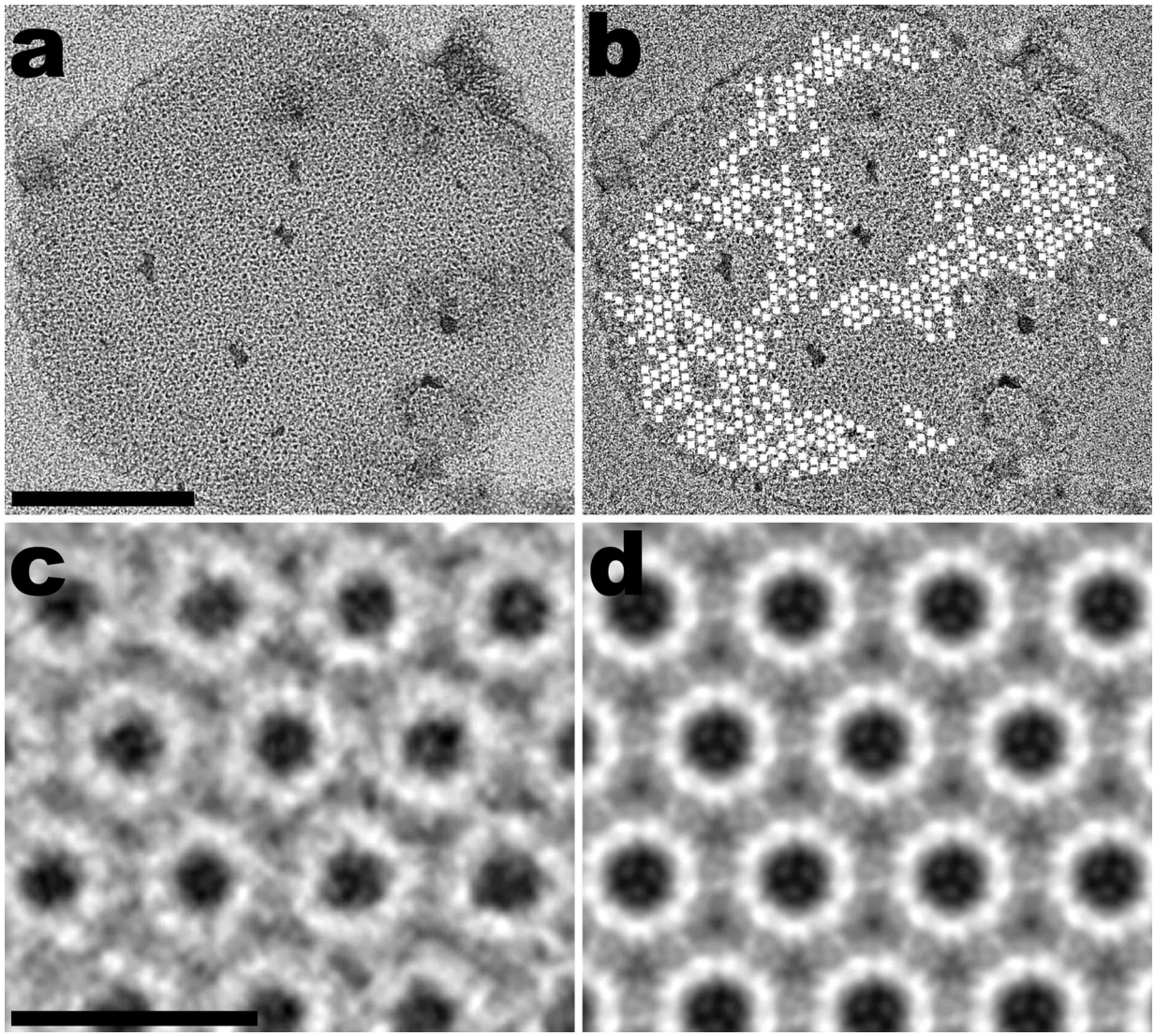

Fig. S2. A 2D crystal of RML prions grown from PTA/PrP 27-30 complexes. (*a*) Raw picture of a 2D crystal before image processing. (*b*) Image of the 2D crystal after CTF correction and high-pass filtering. The lattice positions that were selected for alignment and averaging are indicated with white squares. (*c*) High-power view of the final average after 17 iterative rounds of correlation mapping and averaging. No further improvements could be made at this point because the algorithm had converged. (*d*) Crystallographic average obtained from *c* by applying p3 symmetry. (Scale bar: *a*, 100 nm, and applies to *b*; *c*, 10 nm, and applies to *d*.)

Table S1. Parameters that were tested for their influence on the 2D crystallization of PrP 27-30 from RML-infected brain homogenate

Parameter	Variable
Detergents	Sarkosyl*
	Sodium cholate
	Sodium deoxycholate
	Sodium dioctyl sulfosuccinate
	LDAO
	Brij 97
	Triton X-100
Proteases	Proteinase K*
	Pronase
	Trypsin
Salts	NaCl
	$CuCl_2$
	$MnCl_2$
Chelators	EDTA
Lipids	Crude brain lipids
	Polar brain lipids
Other additives	Glycerol*
	PEG 8000
	Congo red

*Variable that improved the 2D crystallization yield.